Int. J. Electrochem. Sci., 15 **(2020)** 6549 – 6560, doi: 10.20964/2020.07.76

International Journal of
ELECTROCHEMICAL
SCIENCE
www.electrochemsci.org

Enhanced Water Electrolysis: Effect of Temperature on the Oxygen Evolution Reaction at Cobalt Oxide Nanoparticles Modified Glassy Carbon Electrodes

Aya Akl[1], *Hany A. Elazab*[1,2], *Mohamed A. Sadek*[1,*], *Mohamed S. El-Deab*[3]

[1] Department of Chemical Engineering, Faculty of Engineering, The British University in Egypt, Cairo, Egypt.
[2] Nanotechnology Research Centre (NTRC), the British University in Egypt (BUE), El-Sherouk City, Suez Desert Road, Cairo, 11837, Egypt.
[3]Department of Chemistry, Faculty of Science, Cairo University, Cairo, Egypt.
[*]E-mail: shahir.Sadek@bue.edu.eg

Received: 22 December 2019 / *Accepted:* 16 March 2020 / *Published:* 10 June 2020

Water splitting producing hydrogen and oxygen gases appears promising in view of the increasing need of renewable energy sources and storage strategies. Investigation of stable and highly efficient electrocatalysts for oxygen evolution reaction (OER) is targeted in this study at cobalt oxide nanoparticle modified glassy carbon (nano-CoOx/GC) electrodes. The effect of the preparation (T_p) and measuring temperature (T_m) on the electrocatalytic activity of nano-CoOx/GC towards the OER is investigated under various operating conditions. Linear sweep voltammetry (LSV), cyclic voltammetry (CV) as well as SEM and XRD techniques were used to probe the electrocatalytic and morphological characteristics of nano-CoOx prepared under various conditions. Increasing T_p and/or T_m results in improving the kinetics and electrocatalytic activity of the proposed anodes towards the OER as demonstrated in the value of the the onset potential of the OER and the OER currents recorded at a fixed potential. The morphology as well as the surface characterization of the prepared catalyst are reported herein and evaluated.

Keywords: Water splitting, Electrocatalysis, Hydrogen evolution, Nanoparticles, Oxygen evolution

1. INTRODUCTION

The oxygen evolution reaction (OER) is an important reaction in water electrolyzers aiming at the production of high purity hydrogen gas. It has an essential role in electrochemical science and technology as it participates in many necessary applications, e.g., energy storage devices and energy conversion [1-9]. This half-cell reaction (i.e., the OER) is the main source of energy consumption in the industrial water electrolysis processes.

Water electrolysis, for hydrogen production, requires a large amount of energy to drive the reaction by splitting H_2O into H_2 at the cathode and O_2 at the anode. The most important key to increasing the efficiency of the water electrolysis system is to develop highly effective electrocatalysts for the OER [10-14]. An electrocatalyst is a catalyst that is used to accelerate the electrochemical reactions (involving charge transfer across the electrode/electrolyte interface. The electrode surface modification might be achieved via structural and/or (electro)chemical procedures [15-18]. Also, increasing the operating temperature and developing stable and cheap electrocatalysts support high rates of charge transfer [19-23]. Extensive studies have been devoted to develop of efficient electro-catalysts for the OER including metal oxides (RuO_2 and IrO_2 based electrode) [24,25], metalic (Co, Fe, Ni, Mn) [26,27] or hydroxides layers [28,29] and metal oxide carbon nanotubes (CNTs) hybrid catalysts for the OER. The metal oxide based catalysts are relatively poor electrical conductors, thus they are usually supported onto a conducting substrate, e.g., carbon nanotubes (CNTs). This system offers high surface area, corrosion resistant and high conductivity [19], together with enhanced charge transfer for the electrochemical processes at the electrode/electrolyte interface.

Water electrolysis is a process in which water molecule split into oxygen and hydrogen gases electrically. The basic equation of water electrolysis can be described by the following equation:

$$2H_2O \rightarrow 2H_2 + O_2 \quad (1)$$

The overall process consists of oxygen evolution reaction (OER) at the anode and hydrogen evolution reaction (HER) at the cathode of the electrolyzer. OER is more difficult than HER because OER is a four-electron process which is coupled formation of the O−O bond, concurrently with O−H bond splitting (OER in alkaline medium described by Eq. 3). This needs high overpotential to overcome the energy barriers. On the other hand, HER requires only two electrons to generate adsorbed 2 adsorbed H atoms which are subsequently combine to produce H_2 gas molecule. (HER in the alkaline medium described by Eq.2) [30, 31].

$$4H_2O + 4e^- \rightarrow 2H_2 + 4OH^- \quad E^0_c = -0.826\ V \quad (2)$$

$$4OH^- \rightarrow O_2 + 2H_2O + 4e^- \quad E^0_a = 0.404\ V \quad (3)$$

In case of acidic solution (pH close to 0), the processes that occurs at the cathode and anode are described by:

$$2H^+ + 2e^- \rightarrow H_2 \quad E^0_c = 0.0\ V \quad (4)$$

$$2H_2O \rightarrow O_2 + 4H^+ + 4e^- \quad E^0_a = 1.23\ V \quad (5)$$

In neutral solutions (pH close to 7), the HER and OER take place according to:

$$4H_2O + 4e^- \rightarrow 2H_2 + 4OH^- \qquad E^0_c = -0.413\ V \qquad (6)$$

$$2H_2O \rightarrow O_2 + 4H^+ + 4e^- \qquad E^0_a = 0.817\ V \qquad (7)$$

Where E^0_c and E^0_a are the equilibrium half-cell potentials at relevant standard conditions for each case. For water electrolysis, the equilibrium cell potential is 1.23 V at standard conditions. It is relatively preferable to run water electrolysis in acidic or alkaline media due to the ease of charge as well as ions transfer in well-supported electrolytes, e.g., the existence of protons or hydroxide ions, respectively [32].

The aim of the current study is to investigate the influence of the preparation temperature (T_p) of cobalt oxide nanoparticles electrodeposited from aqueous solution onto glassy carbon (nano-CoOx/GC) electrodes towards the OER in alkaline medium at various measurement temperatures (T_m). Electrochemical measurements, e.g., linear sweep voltammetry (LSV) and cyclic voltammetry (CV) were employed to probe the catalytic activity of the proposed anodes towards the OER at various T_p and T_m.

2. EXPERIMENTAL

2.1. Materials, Electrodes, pretreatments, and measurements

All the used chemicals in this study are of analytical grade (purchased from Merck or Sigma-Aldrich) and are used without further purification for the preparation of all solutions by distilled water. Two-compartment three-electrode electrochemical glass cell is used for electrochemical measurements. These measurements are carried out in 0.5M KOH using a Bio-logic SAS potentiostat (model SP-150) operated with EC-lab software. A Pt spiral wire and Ag/AgCl/KCl (sat.) are used as a counter and reference electrodes, respectively. Conventional pretreatment methods are applied to clean the GC electrode (5 mm in diameter) which is served as the working electrode. Typically, the GC electrode is polished with fine emery paper, then with aqueous slurries of fine alumina powder using a polishing micro cloth then washed thoroughly with distilled water to remove any adsorbed alumina particles on the electrode.

2.2 Electrode's modification

Cobalt oxide nanostructures (nano-CoOx) are electrodeposited onto the GC electrode by cyclic voltammetry technique. Typically, the potential is cycled several times (i.e., 10, 20, 30, 40, 50 cycles) in the potential range between 1.2 V and –1.1 V vs. Ag/AgCl/KCl (sat.) at a scan rate of 100 mV s^{-1} in 0.5 M phosphate buffer solution (PBS , pH = 7) containing 2 mM $CoCl_2$. Linear sweep voltammetry (LSV) is used to evaluate the electrocatalytic activity and stability of the nano-CoOx /GC electrodes towards the OER at different preparation and measuring temperatures, T_p and T_m, respectively.

2.3 Materials Characterization

Field emission scanning electron microscope (FE-SEM, QUANTA FEG250) and XRD measurements were employed to disclose the morphology and the crystal structure of the various nano-CoOx/GC electrodes prepared at various T_p.

3. RESULTS AND DISCUSSION:

Fig. 1 shows CVs recorded at various nano-CoOx/GC electrodes (prepared at T_p = 60˚C employing different number of potential cycles) measured in 0.5 M KOH at T_m = 50˚C. The unmodified GC electrode has no significant redox response in the investigated potential range. The formal potential of the redox transformation at 0.24, 0.23, 0.21, 0.16, 0.20 V for 10, 20, 30, 40, 50 cycles. The decrease of the formal potential (towards the negative direction) with CoOx loading (achieved by increasing the number of potential cycles employed for the electrodeposition) refers to enhanced charge transfer activity as result of enrichment of Co-oxide active phase. Moreover, the increase in current intensity of the redox peaks reveals an increase in the surface concentration of the Co-oxide active phases with loading level (c.f. Fig. 9), prior to the onset of the OER. SEM images (shown in Fig. 2) indicate that T_p and loading level of nano-CoOx have marked effects on the morphology and the size of particles of the electrodeposited Co-oxide.

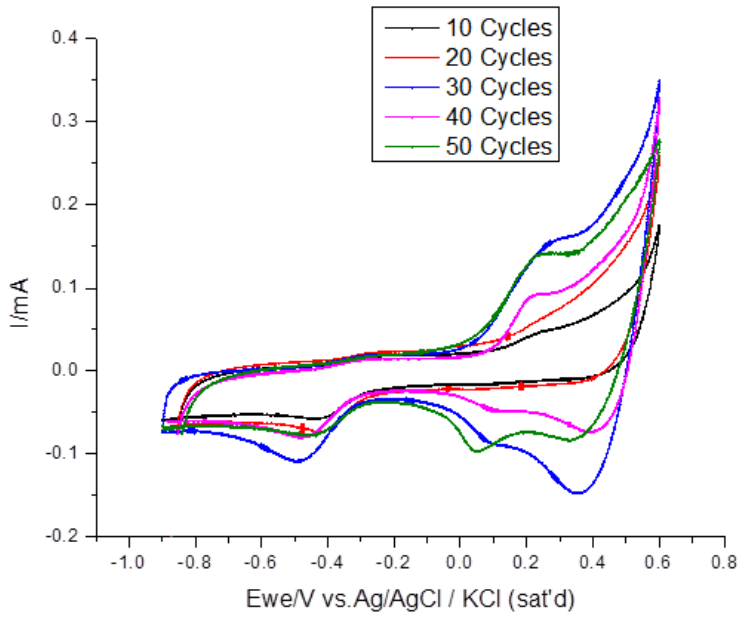

Figure 1 CVs measured at T_m = 50^{0}C for various nano-CoOx/GC electrodes in 0.5 M KOH. Potential scan rate = 200 mV s^{-1}. Note that nano-CoOx are electrodeposited by applying 10, 20, 30, 40, 50 potential cycles (T_p = 60˚C).

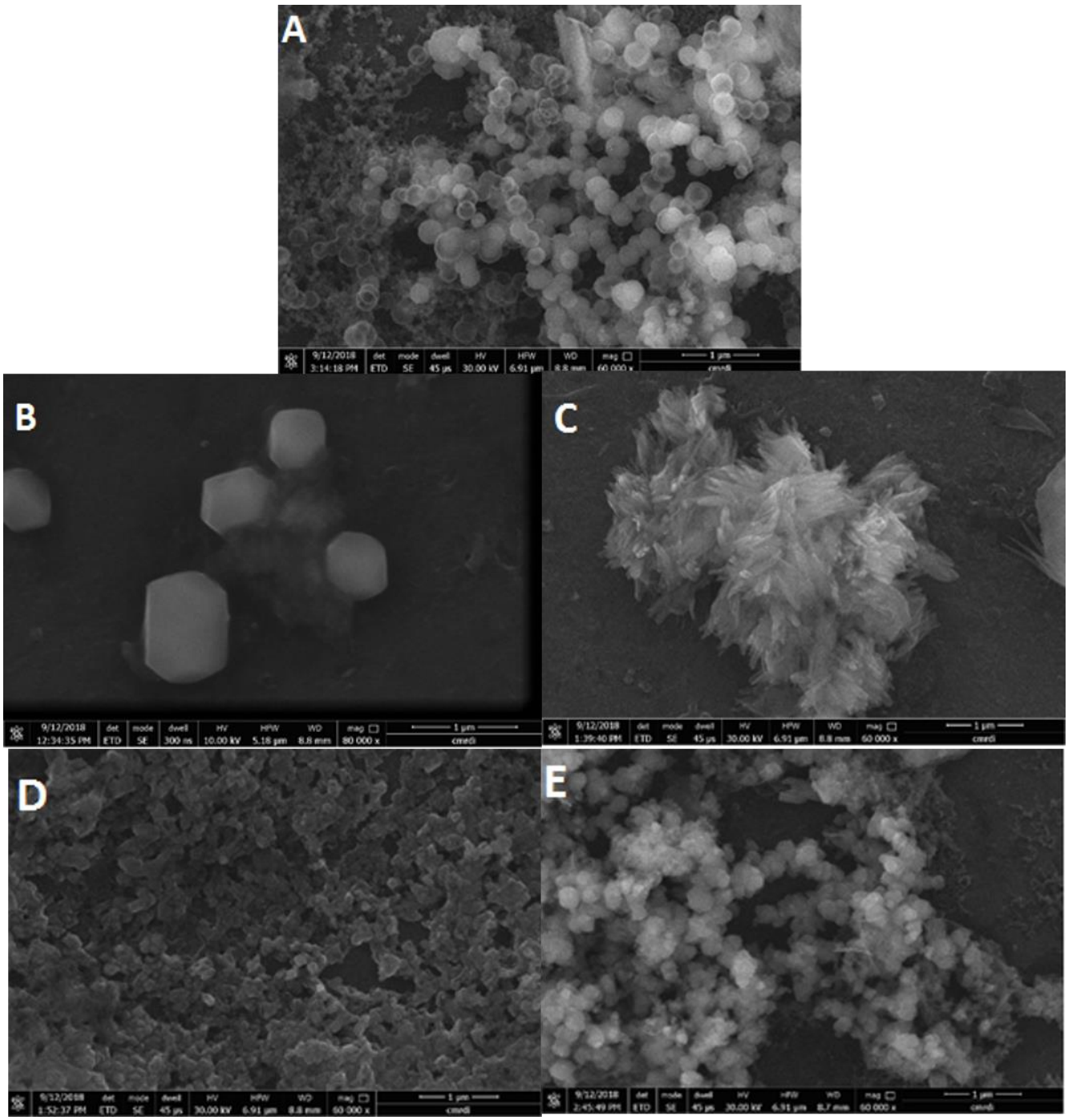

Figure 2 SEM images of nano-CoOx/GC prepared at (A) T_p= 50 ˚C and 40 cycles, (B) T_p= 60 ˚C and 10 cycles, (C and D) T_p= 25 ˚C and 30 cycles and (E) T_p= 60 ˚C and 30 cycles.

This figure shows that a noticeable decrease in the size of particles (at the same loading of CoOx) with increase of T_p, thus leading to a corresponding increase of the active surface area of catalyst. This might explain the increase in the current densities of the redox peaks with no. of cycles observed in Fig. 1.

3.1 Catalytic activity towards the OER:

It is expected that the change of either T_p and/or T_m would result in a corresponding alteration of the kinetics and the catalytic activity of the proposed anodes towards the OER as demonstrated in the value of the exchange current density and the onset potential of the OER. The following section displays the results.

3.1.1 Effect of nano-CoOx loading on the OER:

The catalytic activity of nano-CoOx/GC electrodes towards the OER is investigated by recording LSVs in 0.5 M KOH (prepared employing various number of CV cycles at $T_p = T_m = 25^{\circ}C$), see Fig. 3. For comparison of the catalytic activity of different nano-CoOx/GC electrodes, one can measure the potential at a constant current density or compare the current density at a constant potential.

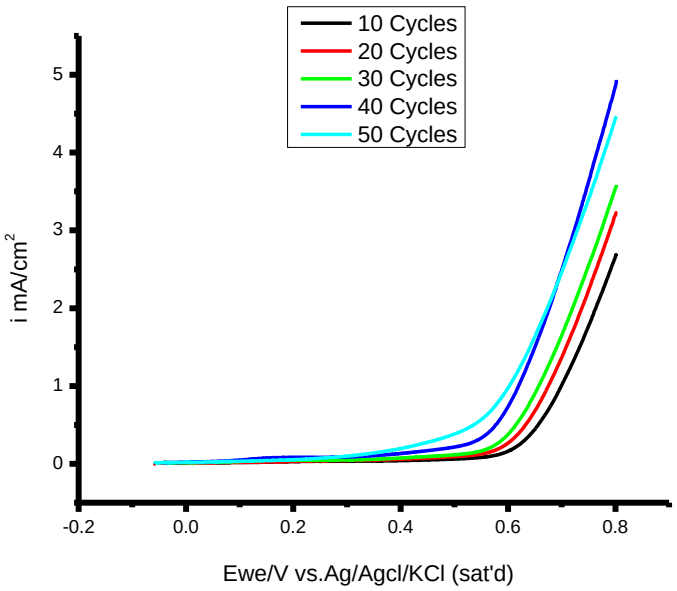

Figure 3. LSVs for the OER at nano-CoOx/GC electrodes (prepared with various number of cycles) measured in 0.5 M KOH at $T_p = T_m = 25^{\circ}C$. Potential scan rate: 20 mVs^{-1}.

A good electrocatalyst should support high OER current density at a low overpotential. The modified nano-CoOx/GC electrodes show a significant increase of current density of the OER measured at $T_p = T_m = 25^{\circ}C$ (prepared by employing 40 potential cycles). Where the current density (recorded at 0.8 V) significantly increases from 2.69 to 3.22, 3.58, 4.93 and 4.46 mA/cm^2 for electrodes prepared by employing 10, 20, 30, 40, 50 potential cycles, respectively. This indicates that the increase of the nano-CoOx loading facilitates the charge transfer during the OER, possibly due to the increase of the population of the active CoOx phases.

3.1.2 Effect of T_m on the OER:

The catalytic activity of nano-CoOx/GC electrodes towards the OER is measured by recording LSVs in 0.5 M KOH at various T_m = 25, 40, 50, 60 ˚C (see Fig. 4). Note that all nano-CoOx/GC electrodes have the same loading level (30 cycles) and are prepared at the same T_p =25 ˚C. Fig. 4 shows that the OER current density measured at 0.8 V is 2.51, 3.58, 3.54 and 4.8 mA/cm^2 at T_m= 25, 40, 50, 60 ˚C, respectively. The OER current measured at T_m= 60 ˚C is the highest. The increase of the solution temperature increases its conductivity and enhances its kinematic viscosity to a favorable level, thus facilitating the ionic mobility and decreases the corresponding overpotential required to support a certain rate of the OER.

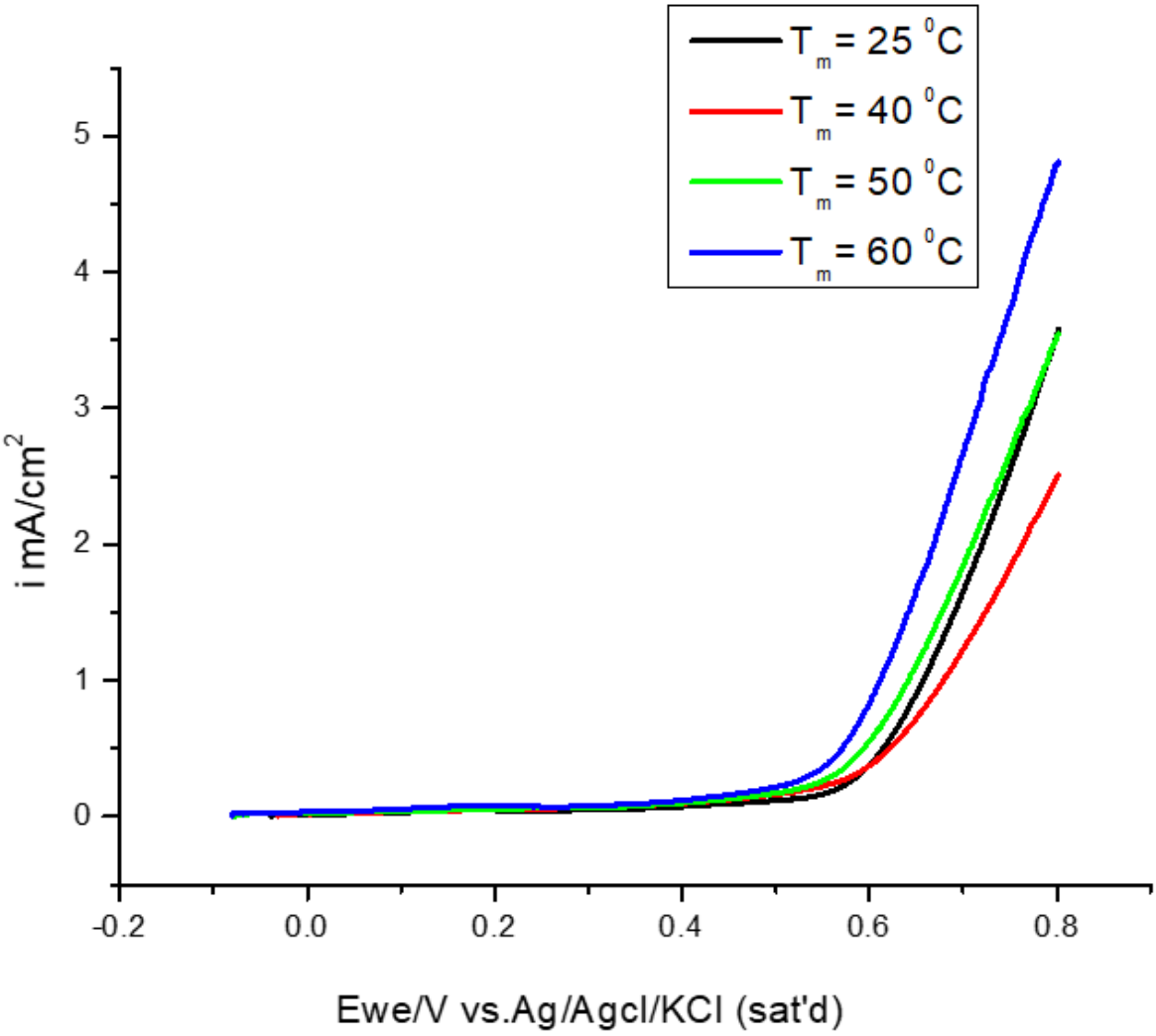

Figure 4. LSVs for the OER at nano-CoOx/GC electrode measured in 0.5 M KOH at various T_m at a constant T_p = 25 ˚C and cycle = 30. Potential scan rate: 20 mV s^{-1}.

3.1.3 Effect of T_P on the OER:

The electrocatalytic activity of nano-CoOx/GC electrodes (prepared by employing 30 potential cycles at various T_P = 25, 40, 50, 60˚C) towards the OER is monitored by recording LSVs in 0.5 M

KOH at constant T_m = 60°C. Fig. 5 shows that the nano-CoOx/GC electrode (prepared at T_p= 60 °C) supports a significant large current density of the OER measured at T_m= 60 ^{0}C. Where current density measured at 0.8 V shifts from 4.8, 2.2, 4.02, 7.9 mA/cm^2 for electrodes prepared at T_p = 25, 40, 50, 60 °C, respectively.

The effect of T_p, T_m and loading level on the electrocatalytic activity of the nano-CoOx/GC electrodes is summarized in Table 1 by reporting the OER current (I_{OER}) in 0.5M KOH measured at overpotential (η) of 180 mV at various CoOx loadings (i.e., 30, 40, 50 cycles, respectively).

Table 1 shows that:

(i) The electrode prepared at T_p= 60 ° C, T_m = 60 °C and constant cycle = 30 shows the highest activity towards OER compared to electrodes cycled at lower T_p.

(ii) The electrode prepared at T_p= 50 ° C, T_m = 50 ° C and constant cycle = 40 shows the highest activity towards OER compared to electrodes cycled at lower T_p.

(iii) The electrode prepared at T_p= 60 ° C, T_m = 60 ° C and constant cycle = 50 shows the highest activity towards OER compared to electrodes cycled at lower T_p.

(iv) At given T_p, the increase of T_m increase I_{OER}.

(v) At given T_m, the increase of T_p from 25° C to 60° C increase I_{OER}.

Table 2 shows a comparison of the obtained results (in the current study) and the reported data using similar cobalt oxide-based nanocatalysts [33-45]. This table reveals good catalytic activity for the proposed CoOx-based catalysts in terms of overpotential.

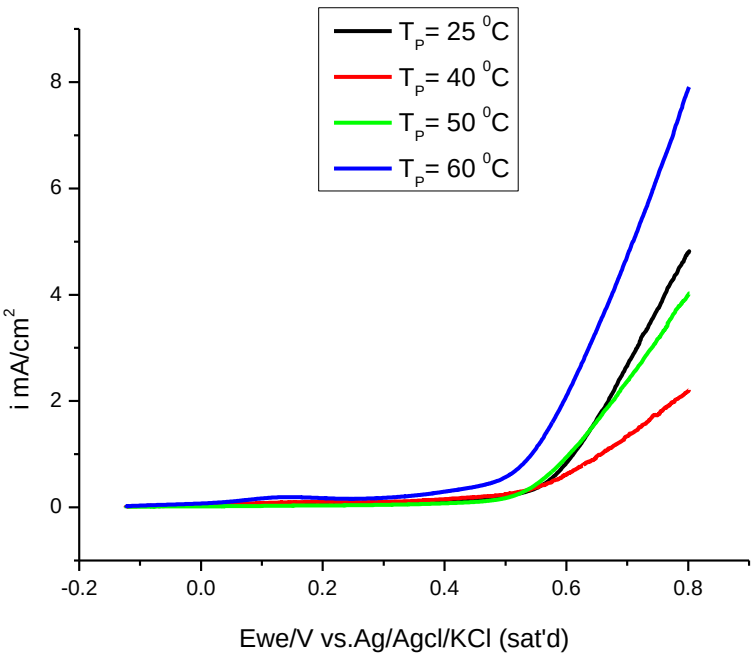

Figure 5. LSVs for the OER at nano-CoOx/GC electrodes measured at constant T_m = 60 ° C in 0.5 M KOH prepared at various T_p= 25, 40, 50, 60 ° C, and cycle= 30. Potential scan rate: 20 mV s^{-1}.

That is the prepared catalyst in the current study has a good catalytic activity towards the OER compared with active catalysts reported in literature. Additionally, the current CoOx nanoparticle-

based catalyst is prepared at milder preparation conditions of the cobalt oxide catalyst. For instance, Liu et al. [34] prepared Co_3O_4 nanoparticle-based electrocatalysts (with various morphologies) at much elevated temperatures (160^{o}C) with a post calcination step (at 300^{o}C for 1-2 h) for application in the OER. This required lots of steps and energy consumption for the preparation of their catalyst. However, our method employed a direct attachment of CoOx atop the surface of the GC substrate via the direct electrodeposition. The ease of preparation of CoOx in our case and the control of its catalytic activity with the preparation temperature (T_p) (in the range from 25 to 60^{o}C) advantageously supports the novelty of our work. Moreover, nano-CoOx/GC electrode (prepared at T_p = 60^{o}C) supports OER current of ca. 8 mA cm^{-2} while polarized at 180 mV (a value which is almost half that reported earlier for CoOx prepared at room temperature [33].

The observed significant catalytic effect of CoOx nanostructures towards the OER could be attributed to the enhanced charge transfer during several elementary steps of the OER in alkaline medium mediated by the redox transformation of the lower oxidation state to the higher oxidation state (see Fig. 1) [46-48]. This reasonably accounts for the increased activity by increasing the loading level of CoOx. Additionally, increasing T_p affects the population of the active phase of CoOx in the catalyst layer (see Figure 6), thus more facilitating effect is noticed. Whereas, T_m increases the conductivity and enhances the ionic mobility, it also affects the charge transfer at the electrode/electrolyte interface in such a way that supports the OER current at lower overpotentials.

Table 1. Variation of the OER current (I_{OER} / mA cm^{-2}) at nano-CoOx/GC electrodes recorded at an overpotential (η) of 180 mV in 0.5 M KOH (at various T_m). Note that CoOx nanoparticles were electrodeposited onto the GC electrode employing various numbers of CV cycles (at various T_p) as described in the experimental part.

I_{OER} / mA cm^{-2}						
T_p / ^{0}C	**T_m/ ^{0}C**	**Number of Potential cycles**				
		10	**20**	**30**	**40**	**50**
25	25	2.7	3.2	3.6	4.9	4.5
40		3.1	2.6	3.0	3.0	3.3
50		2.0	2.4	2.0	2.2	2.7
60		1.4	1.9	2.4	2.9	3.1
25	40	2.7	3.0	2.5	3.0	2.6
	50	3.7	4.0	3.6	3.9	4.2
	60	3.9	2.8	4.8	3.7	4.3
40	40	2.6	2.7	3.5	3.8	4.0
	50	2.0	2.7	2.8	2.9	2.9
	60	2.4	2.9	2.2	4.7	4.8
50	40	1.0	2.1	1.6	2.1	1.9
	50	3.5	3.0	5.0	6.1	4.3

	60	2.0	2.6	4.0	4.0	3.4
60	40	1.9	1.8	5.2	2.9	2.8
	50	2.7	2.7	4.6	2.8	3.5
	60	4.3	4.9	7.9	4.0	5.5

Table 2. Comparison of the electrocatalytic performance of cobalt oxide-based catalysts towards the OER in alkaline media.

Catalyst	Medium	Overpotential (η) / mV	I_{OER} / mA cm^{-2}	Reference
Co_3O_4-1	1 M KOH	308	10	34
Co_3O_4 quantum dots	1 M KOH	270	10	35
Mesoporous Co_3O_4 nanowires	1 M KOH	405	10	36
Co_3O_4/$NiCo_2O_4$ double-shelled nanocages	1 M KOH	340	10	37
Coral-like CoSe	1 M KOH	295	10	38
Co_3O_4-nanoarrays/Ni foam	1 M KOH	310	10	39
Porous Co_3O_4 nanosheets	1 M KOH	368	10	40
Co_3O_4 nanocubes/N-doped graphene	1 M KOH	280	10	41
Nano-CoOx[#]	0.5 M KOH	180	8	This work

[#] Prepared by employing 30 CV cycles for CoOx deposition at T_p = 60ºC.

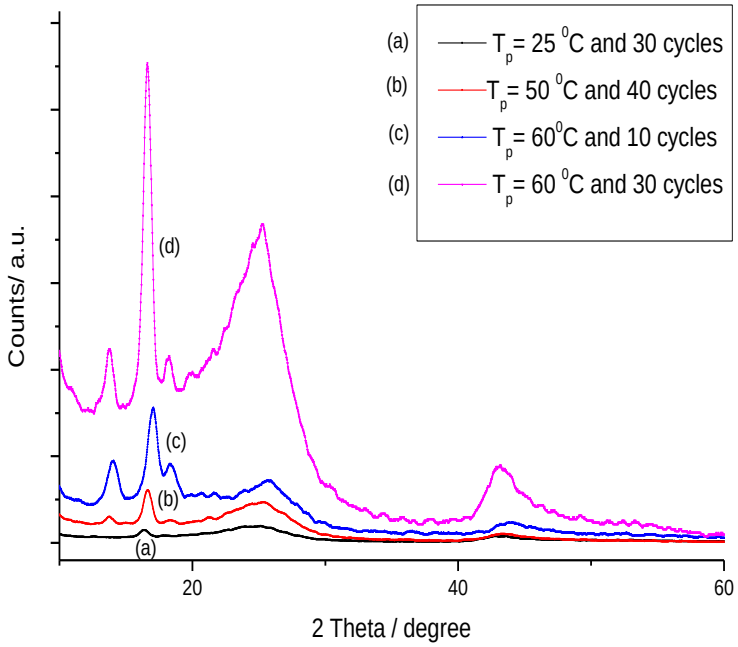

Figure 6. XRD patterns of nano-CoOx modified GC electrodes prepared at various T_p. (a) 25, (b) 50, (c and d) 60˚ C by applying (a and d) 30, (b) 40 and (c) 10 potential cycles between 1.2 V and –1.1 V vs. Ag/AgCl/KCl (sat.) at 100 mV s^{-1}.

4. CONCLUSIONS

Increasing T_p and/or T_m (up to 60^{o}C) results in improving the kinetics and the electrocatalytic activity of the proposed nano-CoOx modified GC anodes towards the OER (in alkaline medium) as demonstrated by the value of the I_{OER} measured at an overpotential of 180 mV and the onset potential of the OER as well. The electrode prepared by employing 30 potential cycles for nano-CoOx electrodeposition at T_p= 60 $^\circ$C shows the highest activity towards the OER (measured in 0.5 M KOH at T_m = 60^{o}C) compared to electrodes prepared at lower T_p This is reasonably attributed to the relative enrichment of the surface with active Co-oxide species which act as catalytic mediator for the several elementary steps of the OER. The proposed anodes in this study show competitive and even better catalytic activity towards the OER compared to those prepared using more sophisticated procedures at higher temperatures.

References

1. L. Collins, K. Bhattacharya, *Structural Multidisciplinary Optimization*, 59 (2019) 389.
2. X. Liu, Z. Yan, and J. Wu, *Appl. Energy*, 15 (2019) 248.
3. R. Magisetty, and N.S. Cheekuramelli, *Appl. Mat. Today*, 14 (2019) 35.
4. M. D. Whale, and E. G. Cravalho, *IEEE Trans. Energy Conversion*, 17 (2002) 130.
5. M.S. Alagha, and P. Szentannai, *Int. J. Heat Mass Transfer*, 1 (2020) 4.
6. W. Yingli, D. Jialong, Z. Yuanyuan, J. Zhengbo, H. Benlin, and T. Qunwei, *Electrochim. Acta*, 20 (2018) 139.
7. Z. Yue, Y. Ya, G. Yousong, Y. Xiaoqin, L. Qingliang, L. Peifeng, Z. Zheng, and W. Zengze, *NanoEnergy*, 14 (2015) 30.
8. Z. Yuanyuan, P. Zhibin, D. Jialong, D. Yanyan, J. Zhengbo, and T. Qunwei, *Energy*, 158 (2018) 555.
9. H. Masahiro, A. Hiroaki, and T. Naoki, *J. Elec. Mat*., (2014), 43, 6, 2196-2201.
10. S. Kim, C. Kim, J. H. Lee, G. Kim, J. Shin, and T. H. Lim, *Electrochim. Acta*, 20 (2017) 399.
11. J. Kotowicz, and M. Jurczyk, *J. Pow. Tech*., 99 (2019) 170.
12. J. W. Yu, G. Jung, Y.-J. Su, C. C. Yeh, M. Y. Kan, C. Y. Lee, and C. J. Lai, *Int. J. Hydrogen Energy*, 44 (2019) 15721.
13. I. B. Pehlivan, M. Edoff, L. Stolt, and T. Edvinsson, *Energy,* 12 (2019) 40.
14. X. Liu, X. Lv, P. Wang, Q. Zhang, B. Huang, Z. Wang, Y. Liu, Z. Zheng, and Y. Dai, *Electrochim. Acta*, 333 (2020) 135488.
15. M. Ishizaki , H. Fujii, K. Toshima, H. Tanno, H. Sutoh, and M. Kurihara, *Inorg. Chim. Acta*, 50 (2020) 119345.
16. C. T. Lu, Y. W. Chiu, M. J. Li, K. L. Hsueh, and J. S. Hung, *Int. J. Electrochem*., 5 (2017) 1.
17. V. R. Chundru, R. Koona, and S. R. Pujari, *Arab. J. Sci. Eng*., 44 (2019) 1425.
18. K. Zeng, and D. Zhang, *Fuel*, 116 (2014) 692.
19. G. Beni, L. M. Schiavone, J. L. Shay, W. C. Smith, and B. S. Schneider, *Nature*, 15 (1979) 281.
20. P. Babar, A.Lokhande, M.Gang, B.Pawar, S. Pawar, and J. Kim, *J. Ind. Eng. Chem*., 60 (2018) 493.
21. Y. Lu, B. Gallant, D. Kwabi, J. Harding, R. Mitchell, M. Whittingham, and Y. Horn, *Energy Environ. Sci.* , 6 (2013) 750.
22. A. Grimaud, K. May, C. Carlton, Y. Lee, M. Risch, W.Hong, J. Zhou, and Y. Horn, *Nature* Commun, 4 (2013) 2439.
23. M. El-Deab, M. Awad, A. Mohammad, and T. Ohsaka, *Electrochem. Commun*., 9 (2007) 2082.

24. S. Bikkarolla, and P. Papakonstantinou, *J. Power Sources* , 28 (2015) 243.
25. H. Wang, Z. Li, G. Li, F. Peng, and H. Yu, *Cat. Today*, 24 (2015) 74.
26. J. Cruz, V. Baglio, S. Siracusano, V. Antonucci, A. S. Arico, R. Ornelas, L. Frade, G. Monreal, S. Duron-Torres, and L. Arriaga, *Int. J. Electrochem. Sci*., 6 (2011) 6607.
27. H. Dau, C. Limberg, T. Reier, M. Risch, S. Roggan, and P. Strasser, *ChemCatChem* , 2 (2010) 724.
28. C. Bocca, A. Barbucci, M. Delucchi, and G. Cerisola, *Int. J. Hydrogen Energy*, 24 (1999) 21.
29. L. Trotochaud, J. Ranney, K. Williams, and S. Boettcher, *J. Am. Chem. Soc*., 13 (2012) 17253.
30. R. Doyle, and M. Lyons, *Phys. Chem*., 15 (2013) 15224.
31. R. Doyle, and M. Lyons, *J. Electrochem. Soc*., 160 (2013) 142.
32. M. Jamesh, and X. Sun, *J. Power Sources*, 40 (2018) 31.
33. I. M. Sadiek, A. M. Mohammad, M. E. El-Shakre, M. I. Awad, M. S. El-Deab, B. E. El-Anadouli, *Int. J. Electrochem. Sci*., 7 (2012) 3350.
34. S. Liu, R. Zhang, W. Lv, F. Kong, W. Wang, *Int. J. Electrochem. Sci*., 13 (2018) 3843.
35. G. X. Zhang, J. Yang, H. Wang, H. B. Chen, J. L. Yang and F. Pan, *ACS Appl. Mater. Inter*., 9 (2017) 16159
36. Y. Wang, T. Zhou, K. Jiang, P. Da, Z. Peng, J. Tang, B. Kong, W. B. Cai, Z. Yang and G. Zheng, *Adv. Energy Mater*., 4 (2014) 1400696.
37. H. Hu, B. Guan, B. Xia and X. W. Lou, *J. Am. Chem. Soc*., 137 (2015) 5590.
38. M. Liao, G. F. Zeng, T. T. Luo, Z. Y. Jin, Y. J. Wang, X. M. Kou and D. Xiao, *Electrochim. Acta*, 194 (2016) 59.
39. J. T. Ren, G. G. Yuan, C. C. Weng and Z. Y. Yuan, *ACS Sustain. Chem. Eng*., 6 (2018) 707.
40. Z. P. Li, X. Y. Yu and U. Paik, *J. Power Sources*, 310 (2016) 41
41. S. K. Singh, V. M. Dhavale and S. Kurungot, *ACS Appl. Mater. Inter*., 7 (2015) 442
42. S. Q. Chen, Y. F. Zhao, B. Sun, Z. M. Ao, X. Q. Xie, Y. Y. Wei and G. X. Wang, *ACS Appl. Mater*. Inter., 7 (2015) 3306.
43. M. J. Liu and J. H. Li, *ACS Appl. Mater. Inter*., 8 (2016) 2158.
44. Z. L. Wu, L. P. Sun, M. Yang, L. H. Huo, H. Zhao and J. C. Grenier, *J. Mater. Chem*. A, 4 (2016) 13534.
45. W. Song, Z. Ren, S. Y. Chen, Y. Meng, S. Biswas, P. Nandi, H. A. Elsen, P. X. Gao and S. L. Suib, *ACS Appl. Mater. Inter*., 8 (2016) 20802.
46. N. Suen, S. Hung, Q. Quan, N. Zhang, Y. Xu, and H. Chen, *Chem. Soc. Rev*., 46 (2017) 337.
47. Y. Cheng, and S. Jiangn, *Nature Sci*., 25 (2015) 545.
48. M. El-Deab, G. El-Nowihy, and A. Mohammad, *Electrochim. Acta*, 165 (2015) 402.